Bamboo and Wood Structures

journal homepage: https://www.innoviair.cn/journal/BWS

Performance-Based Optimal Design of MTMDs for Human-Induced Vibration Serviceability of Glulam Footbridges

Weibao Sun[a,*]

[a]*Nanchang University, Nanchang 330031, China*

ARTICLEINFO

Keywords:
Glued-Laminated Timber
Footbridge Dynamics
Pedestrian Excitation
Vibration Control
Tuned Mass Damper
Multi-Objective Optimization

ABSTRACT

Modern glued-laminated timber (glulam) footbridges, characterized by their slenderness, often feature low stiffness, damping, and modal mass, rendering them susceptible to human-induced vibrations. When primary vibration serviceability requirements are unmet, mitigation measures such as tuned mass dampers (TMDs) are necessary. This paper evaluates the vibration serviceability of a glulam model bridge under realistic pedestrian traffic and presents the optimal design of multiple tuned mass dampers (MTMDs). The model is an approximately 13 m long three-hinged deck arch bridge with two circular arch ribs of 8.7 m radius. The fundamental vertical frequency of the footbridge fell within the critical range specified by recent European guidelines EN 1990 and BS 5400, necessitating further analysis against maximum acceleration thresholds. Beyond peak dynamic responses from pedestrian interaction tests, peak accelerations were calculated per the Chinese guideline JTG D60 and compared with comfort limits. Experimental and analytical results indicate that peak vertical and lateral accelerations of the model bridge must be verified under both single- and crowd-induced loading for the serviceability limit state (SLS). Replacing a moving pedestrian load with fixed-position stepping to excite the footbridge simplifies the solution procedure and yields slightly more conservative results. A genetic algorithm-based optimization method is employed to address the multi-objective optimization problem in MTMD design for reducing human-induced vibrations.

1.Introduction

The impact of pedestrians on footbridges consists of static and dynamic loads. The static load is caused by the pedestrian's weight, while the dynamic load arises from rhythmic body movements, which can induce bridge vibrations. These vibrations can sometimes be significant, potentially compromising the safety and serviceability of the footbridge, and may even lead to serious consequences. One of the earliest recorded failures of a footbridge due to human-induced dynamic loading occurred in Broughton, UK, in April 1831, when 60 soldiers marched in step across the structure [1]. Similarly, the Angers suspension bridge in France, constructed in 1839, experienced excessive vibrations in April 1850 as troops marched over it in unison, ultimately leading to its collapse and the death of 226 people[2]. Although numerous accounts of lively footbridges exist from earlier times[3-7], it was the now-notable swaying of the newly opened London Millennium Bridge on June 10, 2000[8], that drew significant public and professional attention to this issue.

Modern footbridge design increasingly employs lightweight, high-strength materials and longer spans, driven in part by aesthetic demands for slimmer profiles. This trend allows engineers to create more flexible, longer, and lower-frequency bridges, such as contemporary glued-laminated timber (glulam) footbridges. Modern glulam bridges address the limitations of traditional timber structures, combining aesthetics, functionality, and cost-effectiveness. They offer advantages including resource sustainability, environmental

* Corresponding author.
E-mail addresses:weibaosun2001@163.com.
Received 18 September 2025; Received in revised form 29 September 2025; Accepted 05 November 2025; Available online 29 November 2025

friendliness, high strength-to-weight ratio, visual appeal, ease of construction — particularly in alpine regions — as well as resistance to wind, earthquakes, corrosion, fire, and pests, alongside high stability and durability[9,10]. While the static performance of these pedestrian bridges, such as load-bearing capacity and deformation, generally meets structural design and service requirements, their increased flexibility makes them more prone to vibrations under dynamic loading, especially when pedestrians move synchronously. As a result, excessive vibration induced by crowd loading has become a critical design consideration for modern glulam bridges and continues to attract considerable public interest.

The objective of this paper is to evaluate the vibration serviceability of a glulam arch footbridge through experimental and analytical methods. It discusses computational approaches for structural dynamic responses under both single- and multi-pedestrian walking excitations and proposes suitable vibration serviceability limit state (SLS) criteria for such structures. Furthermore, an optimal design method for vibration mitigation using multiple tuned mass dampers (MTMDs) is presented. The effectiveness of this method under various pedestrian excitation scenarios is validated through both experimental testing and analytical simulations.

2.Modelling of Human-Induced Forces

2.1.Single-Person Force Models

The load induced by a single walking pedestrian consists of three force components: a vertical force, generated by the vertical oscillation of the body's center of mass; a lateral force, resulting from the alternating support of the feet; and a longitudinal force, produced by the cyclic action of propulsion and braking. In the time domain, the walking force can berepresented as a summation of Fourier harmonic components[11,12]. While footbridges may also be subjected to other loading conditions such as running and jumping, these types of loads occur less frequently than walking and are therefore not considered in this study.

2.1.1.Dynamic Load Factor (α_i)

Based on measurements of footstep forces, researchers have attempted to quantify Dynamic Load Factors (DLFs), which form the basis for the most commonly used perfectly periodic human-induced force model. Blanchard et al[13] proposed a simple walking-force model considering only the first harmonic for resonance, with a vertical DLF (α_{v1}) of 0.257 and a pedestrian weight of G = 700 N, applicable to footbridges with a vertical fundamental frequency up to 4 Hz. Bachmann and Ammann[14] provided the first five harmonics for vertical walking force and noted that the lateral DLF is approximately one order of magnitude smaller than the vertical one, with the first and third lateral harmonics being dominant ($\alpha_{l1} \approx \alpha_{l3} \approx 0.04$). In contrast, EN1991-2[15] Eurocode 1 specifies a harmonic resonance load with an amplitude of 70 N as the verification load for lateral vibration of footbridges. In the present study, the adopted DLFs for resonant harmonics are $\alpha_{v1} = 0.4$, $\alpha_{v2} = 0.1$, and $\alpha_{l1} = 0.1$.

2.1.2.Walking Frequency (f_p)

The walking frequency of a pedestrian typically ranges from 1.5 to 3.0 Hz, as frequencies above 3 Hz are generally considered running or jumping. Matsumoto et al[16] provided one of the first reliable statistical descriptions of normal walking frequencies based on a sample of 505 individuals, concluding that fp follows a normal distribution with a mean of 2.0 Hz and a standard deviation of 0.173 Hz. Pachi and Ji [16] analyzed 400 random walking samples from two footbridges and also reported a normal distribution for f_p, with a mean of 1.83 Hz and a standard deviation of 0.11 Hz, noting a linear relationship between walking speed and frequency ($v_p \approx 0.71 f_p$). Živanović et al[17] statistically analyzed 2000 walking samples from a footbridge and found that fp follows a normal distribution with a mean of 1.87 Hz and a standard deviation of 0.186 Hz. In this study, analysis of 355 walking samples from college students yielded a normal distribution for f_p with a mean of 1.817 Hz and a standard deviation of 0.14 Hz, which aligns closely with the findings of Chen et al[18]. For the dynamic response calculations under human-induced excitation in this paper, fp is modeled as normally distributed with a mean of 1.825 Hz and a standard deviation of 0.221 Hz.

2.1.3.Phase Shift ($\varnothing_i$)

The phase shift is assumed to follow a uniform distribution between [0, 2π], as the initial step time is not fixed, corresponding to random walking conditions.

2.1.4.Pedestrian Weight (G)

A weight of G = 686 N (calculated as 70 kg × 9.8 m/s²) per person is adopted. Studies indicate that variations in pedestrian weight, which typically follow a normal distribution, have negligible influence on the resulting human-induced vibration responses[19].

2.2.Crowd force models

The mathematical modeling of crowd-induced forces remains challenging, and only a limited number of studies on this topic are available to date. In practice, the analysis method proposed in the HiVoSS[20] guidelines is often adopted to predict human-induced vibration responses. Based on pedestrian density d (pedestrians/m²), the HiVoSS guidelines classify pedestrian traffic into five classes (TC1–TC5) and define four comfort levels (CL1–CL4), ranging from maximum comfort to unacceptable vibration intensity.

To predict the acceleration response, a simplified harmonic load model corresponding to a given pedestrian density d is used for random pedestrian flows. The model determines an equivalent number of fully synchronized pedestrians (N') representing a flow of N random pedestrians, as expressed below (Eq. 1):

$$N' = \begin{cases} 10.8\sqrt{\xi N}, & d < 1\,p/m^2 \\ 1.85\sqrt{N}, & d \geq 1\,p/m^2 \end{cases} \quad (1)$$

where ξ is the structural damping ratio. A uniformly distributed harmonic load corresponding to this equivalent pedestrian stream can then be defined as follows (Eq. 2):

$$P(t)=\mathrm{P}\cos\left(2\pi \mathrm{f_p t}\right)\frac{\mathrm{N}^{'}}{\mathrm{S}}\psi \quad (2)$$

where P is the component of the force generated by a single pedestrian (N), S is the area of the loaded surface (note that $N = S \times d$), f_p is the walking frequency of the pedestrian (Hz), and ψ is the reduction coefficient.

3.Vibration serviceability assessment

To ensure vibration comfort under human-induced loads, two principal approaches exist: shifting away from sensitive frequencies and limiting dynamic responses. The method of avoiding sensitive frequencies is often impractical during the design phase due to considerations of rationality and economy. Consequently, the serviceability limit state (SLS) assessment method, which restricts dynamic responses, is recommended in various national and international specifications[20-29]. This approach requires that the human-induced vibration response of footbridges comply with stipulated human comfort criteria.

3.1.Pedestrian densities

Earlier studies[30] indicate that a single pedestrian walking across a footbridge at its resonant frequency represents the most common form of human-induced vibration, an assumption that has been incorporated into relevant design codes. However, following notable incidents of excessive bridge vibrations induced by crowds—such as those observed on the London Millennium Bridge and the Paris Solferino Bridge since the 1990s—bridge engineers have recognized the need to devote greater attention to the treatment of crowd-induced loading. Currently, based on estimates of pedestrian density during noticeable human-induced vibrations, it is widely accepted that the pedestrian density under such conditions typically ranges from 1.5 to 2.0 persons per square meter. In general, a lower value within this range is adopted, while a higher value may be selected for footbridges located in densely populated areas..

3.2.Vibration SLS criteria

The disparity in individual perception and subjective evaluation standards results in human sensitivity to vibration signals following a certain probability distribution. Consequently, researchers have endeavored to establish a relationship between vibration serviceability limit state (SLS) criteria and subjective comfort evaluation levels. Due to the convenience of measuring acceleration data, quantitative indices such as peak acceleration (a_{max}) and root mean square acceleration (a_{rms}) have been widely adopted for evaluating the comfort level of footbridges.

A comprehensive analysis reveals that the stipulations in the Chinese guideline CJJ 69 regarding the vibration serviceability of footbridges are overly simplistic and no longer meet contemporary design requirements. It is recommended that the peak acceleration (a_{max}), calculated in accordance with the pedestrian loads specified in the Chinese guideline JTG D60[31], be used as the evaluation index for vibration comfort. With reference to the pedestrian comfort criteria provided in recent European guidelines — EN 1990 Annex A2 Eurocode and BS 5400-2 — the maximum acceptable accelerations are defined as follows (Eq. 5 & 6)[32]:

$$a_{max,v} = min\left(0.5\sqrt{f_v}, 0.7\right) \quad (3)$$

$$a_{max,l} = min\left(0.14\sqrt{f_v}, 0.15\right) \quad (4)$$

where $a_{\max,\,v}$ and $a_{\max,\,l}$ are the maximum vertical acceleration and lateral acceleration respectively (m/s^2), f_v and f_l are the fundamental natural frequency of vertical vibration and lateral vibration respectively (Hz).

4.The glulam arch bridge model experiment

4.1.The glulam arch bridge model

The structure is a three-hinged deck arch bridge constructed from larch glulam. The timber components were fabricated by bonding with a single-component polyurethane adhesive under controlled conditions: the moisture content of the larch was maintained between 8% and 15%, with a difference of no more than 5% between adjacent layers; the bonding pressure ranged from 0.6 to 0.8 MPa; ambient temperature was kept between 15℃ and 25℃; and relative humidity was controlled within 50%-70%. On site, all timber elements were connected using steel gusset plates, bolts, and round steel pins to assemble the bridge model, as illustrated in Fig 1. The bridge deck has a clear width of 1 m and a total length of 13.2 m. The calculated arch span is 12.7 m with a rise of 3.0 m, resulting in a rise-to-span ratio of approximately 1:4.2. The superstructure adopts a circular arch configuration with a radius of 8.7 m, consisting of two main arch ribs spaced 0.97 m apart transversely. The two ribs are connected by eight K-type supports, which in turn carry twenty longitudinal columns.

Fig 1. Structural model of the glulam arch bridge

Static load testing confirmed that the bridge model satisfies the design requirement for a crowd load of 3.5 kN/m^2 [33]. For safety and accessibility during testing, steel ladders were installed at both ends of the bridge, and wire-rope guardrails were mounted along the deck.

4.2.Material property tests

In engineering applications, glulam members are manufactured by bonding timber laminations along the grain direction, as the strength of wood is significantly higher parallel to the grain than perpendicular to it. In this study, a series of specimen tests were conducted to determine the material property parameters of the glulam arch bridge. All

specimens were fabricated from the same batch of larch timber. Following the Chinese standards GB/T 1931 and GB/T 1933, twenty standard specimens (20 mm × 20 mm × 20 mm) were tested. The results show that the average moisture content of the larch was 11.43%, and its air-dried density was 0.64 g/cm^3 . The key mechanical properties of the larch are summarized in Table 1.

The material property test results for larch indicate the following:

1) The tensile strength parallel to the grain (f_t) is the highest among the tested properties; however, it is highly sensitive to defects such as knots and cross-grain. Specimens subjected to tensile loading exhibited brittle failure.

2) The compressive strength parallel to the grain (f_c) is the lowest of the tested properties and is only minimally influenced by defects. Specimens under compressive loading failed in a ductile manner.

3) In bending tests, when the compression zone of a specimen reached its ultimate strength, failure did not occur immediately; instead, fine wrinkles appeared. As the bending load increased, these wrinkles expanded further, resulting in relatively large plastic deformation. Final failure occurred when the tensile zone reached its ultimate strength, characterized by rupture of the wood fibers and their inter-fiber bonds. The bending strength parallel to the grain (f_m) of larch is relatively high, approximately 1.5 times that of f_c.

Table 1 Mechanical testing results for larch specimens

Testing types	Testing specimens		Testing results (mean value)				Testing procedures
	length × width ×height (mm)	Quantity	Failure load (kN)	Ultimate strength (MPa)	Elasticity Modulus (GPa)	Poisson's ratio	
Compression test	30 × 20 × 20	15	P_{max} = 20.49	f_c = 50.64	—	—	GB/T 1935 (2009)
Tensile test	follow guidelines	15	P_{max} = 5.34	f_t = 85.50	—	—	GB/T 1938 (2009)
Bending test	300 × 20 × 20	15	P_{max} = 1.82	f_m = 73.23	—	—	GB/T 1936.1 (2009)
	300 × 20 × 20	15	—	—	E = 11.41	μ = 0.36	GB/T 1936.2 (2009)

4.3.Finite- Element based numerical analysis of the human-induced vibration

Based on the maximum acceptable accelerations specified in Eqs. (3)–(4) and the pedestrian loads defined in the JTG D60 guidelines, the human-induced vibration responses of the glulam model bridge were analyzed using the developed finite-element (FE) model. The results provide a reference for the vibration reduction design of footbridges.

4.3.1.The analytical dynamic property of the model bridge

Fig 2. FE model of the glulam arch bridge

A finite-element (FE) model of the glulam model bridge was developed using ANSYS 15.0, as illustrated in Fig 2. The primary structural components were modeled using BEAM189 elements, while pedestrians were represented by MASS21 elements. The complete FE model consisted of 1465 nodes and 784 elements.

Secondary elements such as the bridge deck and guardrail were incorporated as constant loads applied to the main structure. Given the relatively light weight of the timber bridge, the self-weight of the steel connecting members at each joint was considerable and could not be neglected; these were likewise modeled as constant loads applied at the corresponding nodes. In the FE model, the arch footing nodes were treated as rigid connections, reflecting the high stiffness provided by the steel plates and bolts used in the actual connections.

Modal analysis was performed to obtain the natural frequencies and normalized mode shapes (scaled such that the maximum displacement in each mode is unity). In ANSYS, the total kinetic energy of the structure was first calculated, and the modal mass was then derived by dividing this energy by ($\sum\omega^2/2$), where ω is the angular frequency. Table 2 lists the first four computed natural frequencies and corresponding modal masses, and Fig 3 illustrates the associated mode shapes.

The results indicate that the sequence and form of the mode shapes remain unchanged after including pedestrian mass in the model. However, the natural frequencies decrease by 0.8% (one pedestrian), 6.5% (nine pedestrians), and 16.0% (twenty-six pedestrians). This demonstrates that pedestrian mass should be considered in the dynamic response analysis of lightweight glulam footbridges.

When the bridge is unloaded, the fundamental vertical frequency (f_1) is 2.251 Hz, which is below 3.0 Hz. Under full pedestrian load, the fundamental lateral frequency is 3.745 Hz, exceeding 1.2 Hz. It can therefore be concluded that the lateral vibration serviceability of the model bridge meets comfort limits, whereas further analysis is required to evaluate the vertical vibration response against the specified maximum acceleration thresholds.

Table 2 Natural frequencies of the first four orders of the model bridge

Order	Frequency (Hz)				Mode shape	Model mass (no person)
	no person	1 person	9 persons	26 persons		
1	2.251	2.233	2.104	1.891	1st *anti-V*	3603.94
2	4.395	4.360	4.108	3.691	1st *sym-V*	678.30
3	4.459	4.424	4.168	3.745	1st *sym-L*	1336.83
4	6.103	6.055	5.705	5.126	1st *anti-L*	1408.74

Note: *V* vertical bending, *L* lateral bending, *sym-* symmetric, *anti-* anti-symmetric

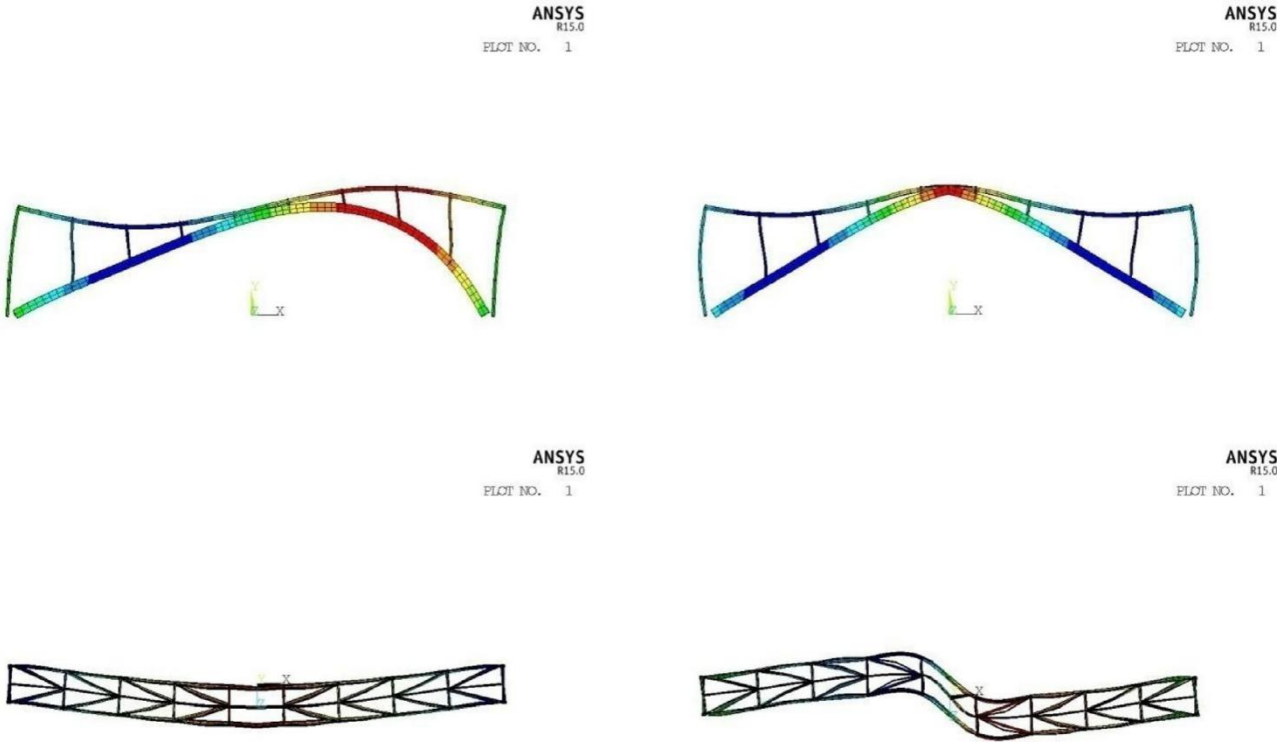

Fig 3. First four mode shapes of the model bridge: (a) the 1st-order anti-symmetric vertical bending mode, (b) the 2nd-order symmetric vertical bending mode, (c) the 3rd-order symmetric lateral bending mode and (d) the 4th-order anti-symmetric lateral bending mode

4.3.2.Human-induced vibration analysis

1) Single pedestrian crossing the bridge

A moving harmonic load was employed to simulate a pedestrian crossing the footbridge at a walking frequency f_p equal to the fundamental vertical frequency f_1, thereby exciting resonance in the corresponding mode. Typically, the first two harmonics are considered potentially resonant; the dynamic force induced by a single pedestrian can be modeled as follows (Eq. 5):

$$P_V(t) = \alpha_{v1} G sin\left(2\pi f_p t + \phi_{v1}\right) + \alpha_{v2} G sin\left(4\pi f_p t + \phi_{v2}\right) \quad (5)$$

where the weight of the pedestrian G is 686 N, the DLF α_{v1} and α_{v2} are 0.4 and 0.1 respectively, and the walking frequency f_p is 2.233 Hz. The measured damping ratio is 1.058%, and the walking speed v_p is set as $0.71 f_p$ (about 1.6 m/s). On the basis of the dynamic response of the FE model, the acceleration-time history at the position of the maximum vertical vibration amplitude (with the distance 3.4 m to the midspan) is shown in Fig 4.

The results indicate that the human-induced vibration response is primarily dominated by the first-order harmonic, as its contribution ($a_{walking}$ = 0.988 m/s^2) accounts for about 90 % of the response from the first two harmonics. Consequently, only the first harmonic of the walking force needs to be considered in the dynamic analysis, i.e., $P_v(t) = 274\sin(2\pi f_p t)$.

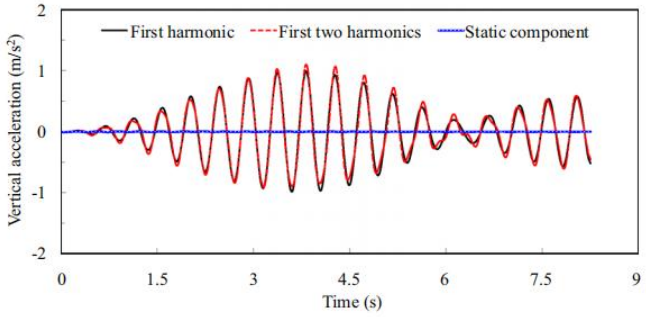

Fig 4. Vertical acceleration-time histories resulting from a pedestrian moving across the model bridge

2) Crowd loading scenarios

According to the design value of maximum pedestrian density d_{max} = 2p/m^2, the total number of pedestrians on the model bridge is 26 ($N = S \times d$ = 13.1m^2 × 2p/m^2). The equivalent pedestrian density n' corresponding to a flow of 26 random pedestrians is calculated as follows:

$$n' = \frac{1.85\sqrt{N}}{S} = 0.72P/m^2 \quad (6)$$

When 26 pedestrians cross the bridge stochastically, the walking frequency f_p is assumed to follow a normal distribution with a mean of 1.825 Hz and a standard deviation of 0.221 Hz, while the initial phase is uniformly distributed over [0, 2π]. A random sampling sequence was generated

based on these distributions, yielding the stochastic stepping excitation for 26 pedestrians: $P_{vi}(t) = 274\sin(2\pi f_{pi}t + \varnothing_{vi})$.

When nine pedestrians (calculated from Eq. 6) step synchronously on the bridge (f_{pi} = 2.104 Hz), pedestrian spacing Δl_p = 1.46 m, the corresponding excitation can be obtained. Both crowd - loading scenarios described above were applied separately to the FE model. In each time step Δt, the position of every pedestrian advances by $v_p \times \Delta t$, and whether pedestrians are entering or leaving the bridge is accounted for.

When pedestrians continuously step onto and off the bridge, the total number on the span remains constant and is uniformly distributed along the entire bridge over a given period. Although the load moves, its effect is equivalent to that produced by pedestrians stepping at fixed positions. Figure 5 presents the acceleration time history at the point of maximum vertical displacement under crowd - induced excitation. The same loading cases were applied in both numerical analyses and experimental tests (see Table 3).

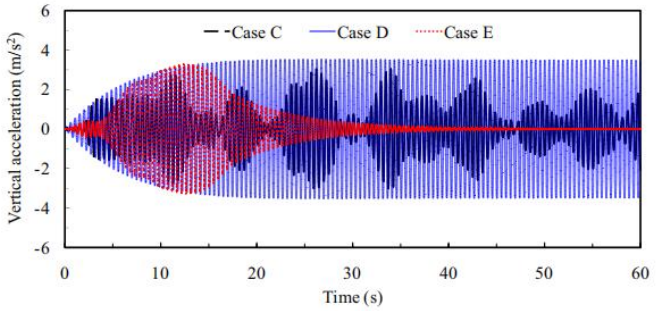

Fig 5. Vertical acceleration-time histories resulting from different crowd induced excitations

3) Comparison of acceleration responses

The peak acceleration under stochastic walking of 26 pedestrians ($a_{max\text{-}26}$ = 3.040 m/s^2) is slightly lower than that under synchronous walking of nine pedestrians ($a_{max\text{-}9}$ = 3.273 m/s^2). This difference occurs because, when considering the actual step - frequency distribution of 26 pedestrians, the number of pedestrians exciting structural resonance is smaller than in the case of nine perfectly synchronized pedestrians.

When nine pedestrians step at fixed positions on the bridge (Δl_p = 1.46 m), the maximum acceleration response (a_{max} = 3.514 m/s^2) is marginally higher than that for nine pedestrians walking synchronously along the bridge. Therefore, for human- induced vibration analysis, equivalent pedestrians can be uniformly placed at fixed deck positions, and the bridge can be excited by in-place stepping to obtain the structure's maximum acceleration response.

4.3.3.SLS assessment for the human-induced vibration

Based on the calculated peak acceleration (a_max) of the model bridge under human-induced excitations, a serviceability limit state (SLS) assessment was conducted (see Table 3). The results indicate that under both single - pedestrian and crowd- induced loading, the vertical vibration of the bridge does not meet the specified comfort requirement. Therefore, vibration mitigation measures are necessary.

Table 3 Vibration serviceability assessment of the model bridge under human-induced excitations

Excitation	Load case	f_1 (Hz)	a_{max} (m/s^2)	a_{limit} (m/s^2)	Comfortable
Single	Case A	2.233	0.988	0.7	No
	Case B	2.233	2.111	0.7	
Crowd	Case C	1.891	3.040	0.688	No
	Case D	2.104	3.514	0.7	
	Case E	2.104	3.273	0.7	

4.4.Optimal design of MTMDs for the model bridge

This paper proposes a vibration mitigation measure using three multiple tuned mass dampers (3-MTMDs) with a total mass ratio of 6%, installed at the location of maximum vertical mode-shape displacement (3.4 m from mid-span). Optimized via a genetic algorithm, the optimal frequency ratio ($f_{di\text{-}opt}$), damping ratio ($\xi_{di\text{-}opt}$), stiffness (k_{di}), and damping coefficient (c_{di}) for each TMD are listed in Table 4. A schematic of the TMD is shown in Fig 6. Due to constraints from diagonal bracing, the centers of the three TMDs are positioned about 15 cm away from the intended design location. Oil-pressure dampers were employed, allowing damping adjustment through piston-area and oil-viscosity control.

Table 4 Optimum parameters of 3-MTMDs

TMD	m_{di}(kg)	$f_{di\text{-}opt}$	$\xi_{di\text{-}opt}$	k_{di}(N/m)	c_{di}(N·s/m)
1	100	0.8560	0.0714	13,346.74	164.97
2	100	0.9467	0.0754	16,324.97	192.68
3	100	1.0582	0.0840	20,396.85	239.93

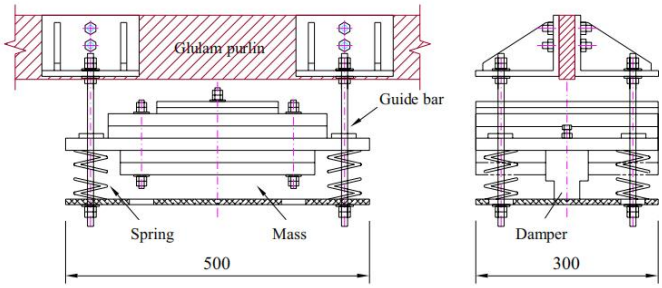

Fig 6. General structural diagram of TMD (Unit: mm)

To evaluate the effectiveness of the 3-MTMD system, the dynamic response of the combined bridge-MTMD system (including the added mass of the MTMDs) was analyzed in ANSYS. The stiffness and damping of each TMD were modeled using COMBIN14 elements, and the TMD mass was represented by MASS21 elements. The real constants for each element were set according to Table 3. Under a single moving load (G = 684 N, f_p = 2 Hz, v_p = 1.5 m/s), the simulated maximum displacement and acceleration align closely with measured values (Fig 7), confirming the rationality of the designed MTMD parameters and the human-induced load model.

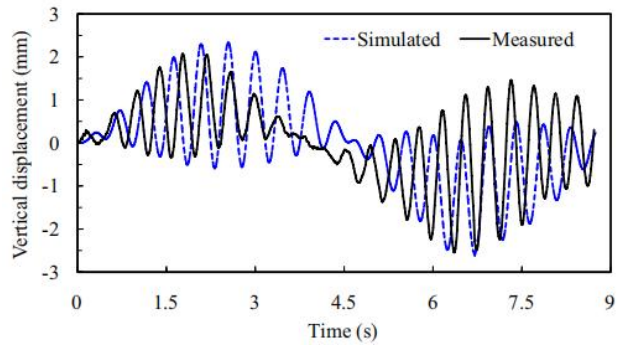

(a) displacement–time histories

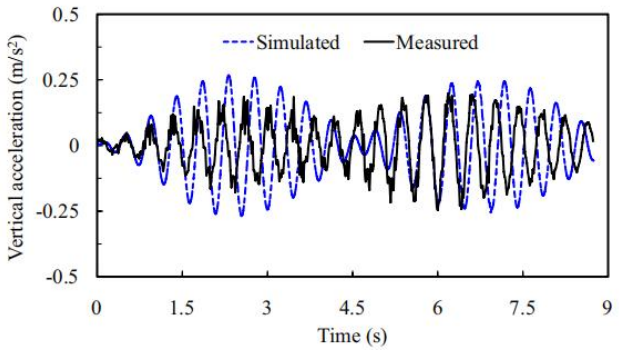

(b) accelerationtime histories

Fig 7. Dynamic responses resulting from a pedestrian moving across the model bridge

Figure 8 compares the acceleration time histories at the point of maximum vertical displacement before and after TMD installation under different loading cases. Compared to a single TMD with the same total mass ratio of 6%, the 3-MTMD system improves vibration-reduction efficiency by an average of 10.8% across various load conditions. For a single-degree-of-freedom system equipped with MTMDs, Fig. 2b indicates that 3-MTMDs achieve a 10.9% higher efficiency than a single TMD. The improvement calculated in ANSYS closely matches that of the idealized single-degree-of-freedom system, demonstrating the feasibility of placing three optimized TMDs at the maximum amplitude of the target mode to effectively mitigate footbridge vibrations.

The results show that the proposed 3-MTMD system effectively controls large-amplitude vibrations of the model bridge, achieving a reduction of approximately 72.7% to 85.9%. After installation, the maximum acceleration responses decrease from 2.111m/s^2 (single-pedestrian load) and 3.514m/s^2 (crowd load) to 0.298m/s^2 and 0.679m/s^2, respectively—both below the specified comfort limits. This confirms that the dynamic response of the bridge with 3-MTMDs satisfies vibration serviceability requirements.

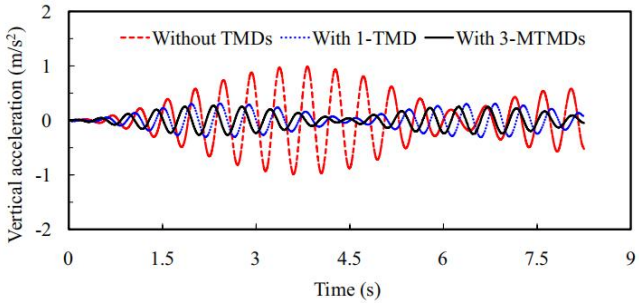

(a)

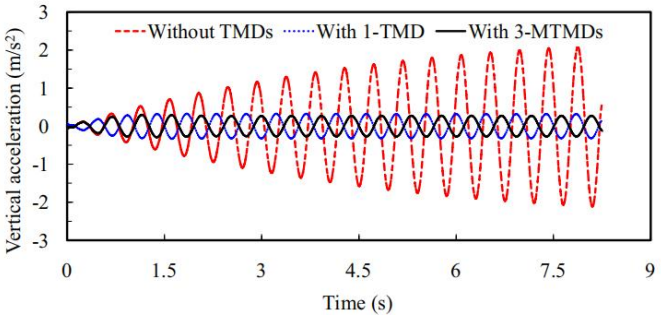

(b)

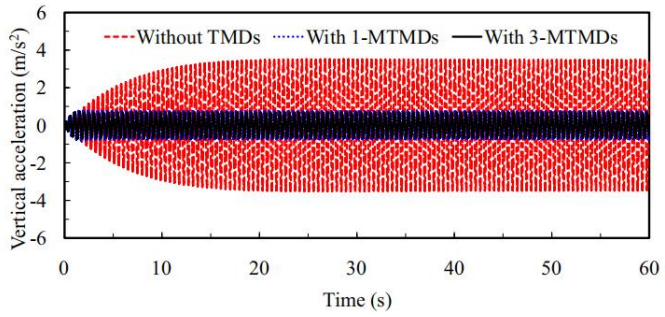

(c)

Fig 8. Analytical vertical acceleration-time histories in different loading cases: (a) Case A, (b) Case B and (c) Case D

5.Conclusions

Glulam footbridges are often highly flexible structures susceptible to human- induced vibrations, making vibration serviceability assessment essential during the design phase. This paper evaluates the serviceability of a glulam model bridge through experimental and analytical investigations. The study found that the fundamental vertical frequency of the bridge fell within a critical range, warranting further dynamic analysis. Consequently, dynamic tests were performed to assess the maximum acceleration response under various pedestrian loading scenarios, with groups of pedestrians walking along the entire bridge. The measured peak accelerations exceeded the comfort limits under all loading conditions, leading to the proposal of a vibration mitigation strategy using three multiple tuned mass dampers (3 - MTMDs). The following results indicate that, after installation of the 3 - MTMDs, the dynamic response of the bridge satisfies vibration serviceability requirements.

(1) Pedestrian mass should be considered in the dynamic response analysis of lightweight glulam footbridges.

(2) Replacing moving pedestrian loads with fixed - position stepping simplifies the solution procedure and yields slightly conservative (safer) results.

(3) Optimally designed non - uniformly distributed 3 - MTMDs can effectively control the vibration response of a glulam footbridge within a narrow resonance frequency band. The vibration reduction effect is most pronounced when both the mass ratio and damping ratio are relatively small, demonstrating favorable economic applicability of MTMDs.

(4) The improvement in vibration reduction efficiency achieved by using 3 - MTMDs compared to a single TMD with the same total mass ratio is modest, amounting to approximately 10%.

(5) A genetic- algorithm- based optimization method can be effectively applied to the multi - objective design of MTMDs for mitigating human- induced vibrations. The 3- MTMD system designed in this study, with a total mass ratio of 6%, reduces the peak vertical acceleration response of the model bridge from 2.803 m/s² to 0.634 m/s².

References

[1] TILLY G P, CULLINGTON D W, EYRE R. Dynamic Behaviour of Footbridges. Construction, 1984, 26(84): 13 – 24.

[2] PETERS T F. Transitions in Engineering: Guillaume Henri Dufour and the Early 19th Century Cable Suspension Bridges. Basel, Switzerland: Birkhäuser Verlag, 1987.

[3] FUJINO Y, PACHECO B M, NAKAMURA S I, et al. Synchronization of Human Walking Observed During Lateral Vibration of a Congested Pedestrian Bridge. Earthquake Engineering & Structural Dynamics, 1993, 22(9): 741 – 758.

[4] BLEKHERMAN A N. Autoparametric Resonance in a Pedestrian Steel Arch Bridge: Solferino Bridge, Paris. Journal of Bridge Engineering, 2007, 12(6): 669 – 676.

[5] NIMMEN K V, BROECK P V, LOMBAERT G, et al. Pedestrian-Induced Vibrations of Footbridges: An Extended Spectral Approach. Journal of Bridge Engineering, 2020, 25(8): 04020058.

[6] INGÓLFSSON E T, GEORGAKIS C T, JÖNSSON J. Pedestrian-Induced Lateral Vibrations of Footbridges: A Literature Review. Engineering Structures, 2012, 45: 21 – 52.

[7] BAAS E J, RIGGIO M, BARBOSA A R. Structural Health Monitoring Data Collected During Construction of a Mass-Timber Building with a Data Platform for Analysis. Data in Brief, 2021, 35: 106845.

[8] HAO J X, WU X F, OPORTO G, et al. Structural Analysis and Strength-to-Weight Optimization of Wood-Based Sandwich Composite with Honeycomb Core Under Three-Point Flexural Test. European Journal of Wood and Wood Products, 2020, 78: 1195 – 1207.

[9] LIEVENS K, LOMBAERT G, ROECK G, et al. Robust Design of a TMD for the Vibration Serviceability of a Footbridge. Engineering Structures, 2016, 123: 408 – 418.

[10] CAPRANI C C, AHMADI E. Formulation of Human – Structure Interaction System Models for Vertical Vibration. Journal of Sound and Vibration, 2016, 377: 346 – 367.

[11] BLANCHARD J, DAVIES B L, SMITH J W. Design Criteria and Analysis for Dynamic Loading of Footbridges//Proceedings of a Symposium on Dynamic Behaviour of Bridges at the Transport and Road Research Laboratory. Berkshire, UK: Transport and Road Research Laboratory, 1977.

[12] BACHMANN H, AMMANN W. Vibrations in Structures Induced by Man and Machines. Zürich, Switzerland: International Association for Bridge and Structural Engineering, 1987.

[13] EUROPEAN COMMITTEE FOR STANDARDIZATION. *Eurocode 1: Actions on Structures – Part 2: Traffic Loads on Bridges: EN 1991-2. Brussels, Belgium: European Committee for Standardization, 2003.

[14] MATSUMOTO Y, SHIOJIRI H, NISHIOKA T. Dynamic Design of Footbridges//Proceedings of the International Association for Bridge and Structural Engineering. Zürich, Switzerland: International Association for Bridge and Structural Engineering, 1978.

[15] PACHI A, JI T J. Frequency and Velocity of People Walking. The Structural Engineer, 2005, 83(3): 36 – 40.

[16] ŽIVANOVIĆ S, PAVIĆ A, REYNOLDS P. Probability-Based Prediction of Multi-mode Vibration Response to Walking Excitation. Engineering Structures, 2007, 29(6): 942 – 954.

[17] CHEN Z Q, HUA X G. Vibration and Dynamic Design of Footbridges. Beijing, China: China Communication Press, 2009.

[18] BRUNO L, CORBETTA A. Uncertainties in Crowd Dynamic Loading of Footbridges: A Novel Multi-scale Model of Pedestrian Traffic. Engineering Structures, 2017, 147: 545 – 566.

[19] HUMAN INDUCED VIBRATIONS OF STEEL STRUCTURES (HIVOSS). Design of Footbridges: Guideline. Brussels, Belgium: Research Fund for Coal and Steel Publications, 2008.

[20] BRITISH STANDARDS INSTITUTION. *Steel, Concrete and Composite Bridges – Part 2: Specification for Loads: BS 5400-2. London, UK: British Standards Institution, 2006.

[21] EUROPEAN COMMITTEE FOR STANDARDIZATION. *Eurocode: Basis of Structural Design – Annex A2: Application for Bridges: EN 1990-Annex A2. Brussels, Belgium: European Committee for Standardization, 2005.

[22] EUROPEAN COMMITTEE FOR STANDARDIZATION. *Eurocode 5: Design of Timber Structures – Part 2: Bridges: EN 1995-2. Brussels, Belgium: European Committee for Standardization, 2004.

[23] CANADIAN STANDARDS ASSOCIATION. *Canadian Highway Bridge Design Code: CSA S6-14. Mississauga, Canada: Canadian Standards Association, 2014.

[24] GENERAL ADMINISTRATION OF QUALITY SUPERVISION, INSPECTION AND QUARANTINE OF THE PEOPLE'S REPUBLIC OF CHINA. *Mechanical Vibration and Shock – Evaluation of Human Exposure to Whole-Body Vibration – Part 1: General Requirements: GB/T 13441.1-2007. Beijing, China: Standards Press of China, 2007.

[25] MINISTRY OF CONSTRUCTION OF CHINA. *Technical Specifications for Urban Pedestrian Overcrossing and Underpass: CJJ 69-95. Beijing, China: China Architecture & Building Press, 1996.

[26] NIMMEN K V, LOMBAERT G, ROECK G, et al. Vibration Serviceability of Footbridges: Evaluation of the Current Codes of Practice. Engineering Structures, 2014, 59: 448 – 461.

[27] FERRAROTTI A, TUBINO F. Generalized Equivalent Spectral Model for Vibration Serviceability Analysis of Footbridges. Journal of Bridge Engineering, 2016, 21(12): 04016091.

[28] RICCIARDELLI F, DEMARTINO C. Design of Footbridges Against Pedestrian-Induced Vibrations. Journal of Bridge Engineering, 2016, 21(8): C4015003.

[29] JTG D60-2015. General Specifications for Design of Highway Bridges and Culverts. Beijing, China: Ministry of Transport of China, 2015.

[30] TUBINO F, PICCARDO G. Serviceability Assessment of Footbridges in Unrestricted Pedestrian Traffic Conditions. Structure and Infrastructure Engineering, 2016, 12(12): 1650 – 1660.

[31] QU B. Study on Static Performance of Glulam Arch Bridge. Changsha, China: Central South University of Forestry & Technology, 2017.